

Connection between new particle formation and sulphuric acid at Hohenpeissenberg (Germany) including the influence of organic compounds

Pauli Paasonen¹⁾, Sanna-Liisa Sihto¹⁾, Tuomo Nieminen¹⁾,
Henri Vuollekoski¹⁾, Ilona Riipinen¹⁾, Christian Plaß-Dülmer²⁾,
Harald Berresheim²⁾³⁾, Wolfram Birmili⁴⁾ and Markku Kulmala¹⁾

¹⁾ Department of Physics, P.O. Box 64, FI-00014 University of Helsinki, Finland

²⁾ German Weather Service, Meteorological Observatory Hohenpeissenberg, Albin Schwaiger Weg 10, D-82383 Hohenpeissenberg, Germany

³⁾ present address: Department of Physics, Environmental Change Institute, National University of Ireland, Galway, Co. Galway, Ireland

⁴⁾ Leibniz Institute for Tropospheric Research, Permoserstrasse 15, D-04318 Leipzig, Germany

Received 18 Dec. 2008, accepted 23 Feb. 2009 (Editor in charge of this article: Veli-Matti Kerminen)

Paasonen, P., Sihto, S.-L., Nieminen, T., Vuollekoski, H., Riipinen, I., Plaß-Dülmer, C., Berresheim, H., Birmili, W. & Kulmala, M. 2009: Connection between new particle formation and sulphuric acid at Hohenpeissenberg (Germany) including the influence of organic compounds. *Boreal Env. Res.* 14: 616–629.

We analysed the coupling of atmospheric particle formation and sulphuric acid during the Hohenpeissenberg Aerosol Formation Experiment (HAFEX) carried out in 1998–2000. A clear correlation between the particle formation rate and the sulphuric acid concentration to the power from one to two was identified. For each of the analysed 45 particle formation days, we evaluated the coefficients quantifying this coupling in activation and kinetic nucleation theories, predicting linear and squared dependencies, respectively. The median activation and kinetic coefficients were $1.6 \times 10^{-7} \text{ s}^{-1}$ and $3.2 \times 10^{-14} \text{ cm}^3 \text{ s}^{-1}$. The daily values of the coefficients varied within two orders of magnitude and, even during one day, the observed formation rates fluctuated around the predicted rates. A squared dependency was almost as frequent as linear, but the kinetic coefficient anticorrelated with sulphuric acid concentration. This anticorrelation and the variation of the coefficients could be related to the observed correlation between the coefficients and monoterpene oxidation product concentrations.

Introduction

Fine and ultrafine particles exert a significant influence on the earth's radiative balance and thus climate (e.g. Ramanathan *et al.* 2007). This climate influence is commonly divided in two: the direct effect arises because particles reflect and absorb solar radiation, and the indirect effect is due to their impact on cloud formation. Both

reflecting and cloud forming features decrease the radiative forcing on earth whereas the absorbing effect increases it; in total the aerosol effect is estimated to be negative (IPCC 2007). Additionally, atmospheric particulate matter is known to affect human health (Dockery and Pope 1994, Pope *et al.* 2002) and reduce visibility (Cabada *et al.* 2004).

Nucleation, the process in which new particles are formed from vapours, is a significant

source of particles in atmosphere (Spracklen *et al.* 2006). New particles are formed through nucleation on a local scale, such as in trace gases released from combustion processes, but also on a larger, regional scale. Typically during a regional nucleation event the new particle formation rate is increased for a couple of hours in an area of several hundreds of square kilometres. Regional nucleation events have been observed throughout the world (Kulmala *et al.* 2004a), with the corresponding particle formation and growth rates varying by several orders of magnitude. Regional nucleation events can occur in metropolitan areas as well as in clean natural environments with different kinds of vegetation, ranging from polar to tropical climate.

Sulphuric acid has been identified as a key component related to observations of new particle formation and growth (e.g. Weber *et al.* 1995) and many different nucleation theories involving sulphuric acid have been proposed. Classical theories of binary (sulphuric acid–water, Vehkamäki *et al.* 2002) and ternary (sulphuric acid–ammonia–water; Napari *et al.* 2002) nucleation are not able to predict observed nucleation rates in atmospheric boundary layer, even though in free troposphere they work reasonably well (Spracklen *et al.* 2008). Especially, binary and ternary nucleation theories fail to reproduce the observation that nucleation rate is correlated with sulphuric acid concentration to the power of 1–2 (Sihto *et al.* 2009). To explain the observed correlations, the so-called activation and kinetic nucleation mechanisms have been proposed (Weber *et al.* 1997, Kulmala *et al.* 2006). These theories involve empirical nucleation coefficients, which have been reported for a boreal forest site (Sihto *et al.* 2006), a semi-urban site in Germany (Riipinen *et al.* 2007), and a rural site in USA (Kuang *et al.* 2008). The question remaining has been the reason for the great variability of the nucleation coefficients: the coefficients vary over two orders of magnitude at a particular observation site.

In this article, we extend the previous work on activation and kinetic nucleation mechanisms by analysing the coupling of the nucleation rate and sulphuric acid concentration at Hohenpeissenberg, a rural site in southern Germany. The measured nucleation rates are compared with

those predicted by the activation and the kinetic theories, and nucleation coefficients are determined. The results are compared with the previous studies from the boreal forest site in Hyytiälä, Finland, and the semi-urban site in Heidelberg, Germany. In terms of anthropogenic pollution, Hohenpeissenberg ranges between the conditions reported for Hyytiälä and Heidelberg. In addition, the Hohenpeissenberg data set includes nucleation events throughout the year, whereas previous studies used data from spring-time campaigns only. The analysis of this long-term data set was particularly useful with respect to elucidating the considerable variations in the nucleation coefficients observed in the former studies. Both the daily and momentary nucleation coefficients were compared with measured meteorological variables, trace gas concentrations and concentrations of various volatile organic compounds (VOCs). Because there may be other components than sulphuric acid taking part in the nucleation process, we also investigated the correlation of the nucleation rate with the concentration of the hydroxyl radical.

Measurements

During the Hohenpeissenberg Aerosol Formation Experiment (HAFEX), extensive measurements of aerosol particles and trace gases were made between April 1998 and August 2000 at the Hohenpeissenberg Meteorological Observatory, operated by the German National Meteorological Service (DWD). The observatory is located on the Hohenpeissenberg mountain (980 m a.s.l.) about 40 km north of the Alps in southern Germany. The mountain resides 300 m above the surrounding countryside, and lies 500 m north-east of the Hohenpeissenberg village (778 m a.s.l.). Except for the nearby village, the surroundings of the observatory are mainly forest and meadows.

The HAFEX data set includes the particle size distribution, the gas-phase concentrations of sulphuric acid and hydroxyl radicals, and numerous additional routine-measured trace gases and meteorological parameters (Birmili *et al.* 2003). The particle size distributions were recorded with a Differential Mobility Particle Sizer (DMPS) having 39 size classes with mobility diameters

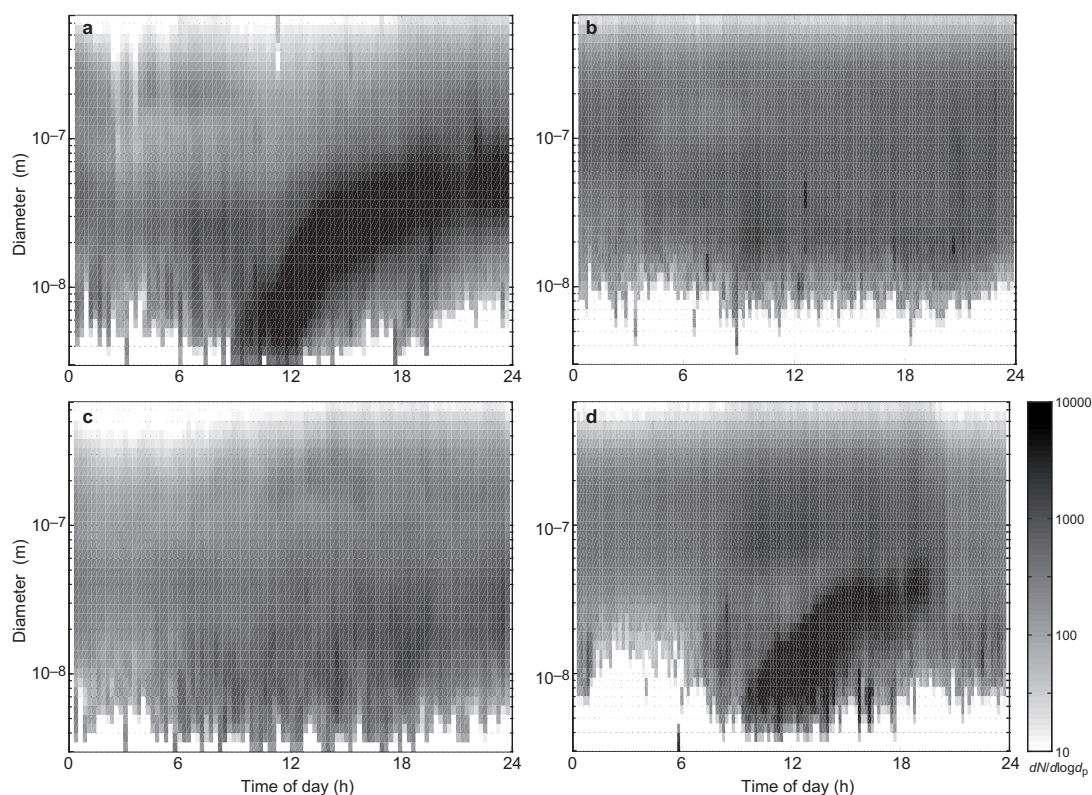


Fig. 1. An example of particle size distribution measured with DMPS on (a) a nucleation event day (14 Apr. 1999), (b) a typical non-event day (26 May 2000), (c) a non-event day (16 Sep. 1998) when the wind was blowing from the Hohenpeissenberg village, and (d) a nucleation event day (17 May 2000) when the event was not clearly observed in the two smallest size channels of the DMPS.

in the range 3–800 nm and the time resolution of 10 minutes (Birmili *et al.* 1999). The gaseous sulphuric acid and hydroxyl radical concentrations were measured with a five-minute time resolution with AP-CIMS (Atmospheric Pressure Chemical Ionization Mass Spectrometer; Berresheim *et al.* 2000). Monoterpene and aromatic hydrocarbon concentrations were determined by gas chromatography ion-trap mass spectrometer (GC-MS) measuring 20 minute average concentrations hourly. An extensive phenomenological account of the HAFEX measurement data can be found in Birmili *et al.* (2003).

Data analysis

Classification of the days

All the days when the particle size distribu-

tion data were sufficient, were classified into either particle formation events, non-events, or undefined days. The classification was made visually according to the criteria presented by Dal Maso *et al.* (2005). However, these criteria were initially developed for a measurement place with no other significant sources of nucleation mode particles than atmospheric nucleation. According to Dal Maso *et al.* (2005), the days when a new nucleation mode (particle diameter < 25 nm) appears and the growth of the mode diameter is observed, are classified as particle formation event days (*see example in Fig. 1a*). The days when nucleation mode particles are not observed, are classified as non-event days (*see example in Fig. 1b*). Other days, for instance days with appearing nucleation mode particles but no subsequent growth, are to be classified as undefined. However, in Hohenpeissenberg a new mode with constant mean diameter of around

10 nm was often observed when the wind was blowing from the village direction (see example in Fig. 1c). This mode was likely to be of local anthropogenic origin, since the continuous growth of the particles was not seen and the mode was observed always between 06:00 and 18:00. Thus, in this study this kind of days were classified as non-events, because they showed no signs of regional new particle formation event.

Determination of time delay Δt and growth rate GR

The particle size distributions used in this study were measured with DMPS detecting only particles with a diameter ≥ 3 nm. According to recent observations (Kulmala *et al.* 2007), the diameter of the nucleating particles is around 1.5 nm. Thus, the freshly nucleated particles were not observed at the time of their formation but after a time interval Δt , during which they had grown enough to achieve the diameter of 3 nm.

Assuming that a change in sulphuric acid concentration $[\text{H}_2\text{SO}_4]$ leads practically instantaneously to a change in nucleation rate, we took the time difference between the observed changes in $[\text{H}_2\text{SO}_4]$ and N_{3-6} to represent Δt .

The growth rate $\text{GR}_{1.5-3}$ from the nucleation size to the detectable size was calculated from the time delay Δt with the formula

$$\text{GR}_{1.5-3} = \frac{3 \text{ nm} - 1.5 \text{ nm}}{\Delta t} = \frac{1.5 \text{ nm}}{\Delta t}. \quad (1)$$

We used this constant growth rate to represent the growth of freshly nucleated particles during the whole day. This assumption does not necessarily hold in all cases, but a more accurate estimation of the growth rate for particles with a diameter < 3 nm was not available.

To estimate the fraction of the growth rate which can be explained by sulphuric acid, $\text{GR}_{1.5-3}$ calculated with Eq. 1 was compared with the theoretical growth rate corresponding to the observed $[\text{H}_2\text{SO}_4]$. The growth rate due to H_2SO_4 was calculated by using the procedure by Kulmala *et al.* (2001)

$$\text{GR}_{\text{H}_2\text{SO}_4} = \frac{1 \text{ nm h}^{-1}}{1.36 \times 10^7 \text{ cm}^{-3}} [\text{H}_2\text{SO}_4], \quad (2)$$

where $1.36 \times 10^7 \text{ cm}^{-3}$ is the sulphuric acid concentration corresponding to a growth rate of 1 nm h^{-1} . Equation 2 is derived for particles with diameters significantly larger than the dimensions of the condensing vapour. Lehtinen and Kulmala (2003) reported that condensation is enhanced at small particle sizes, leading to an enhancement factor between 2 and 3 for 1–3 nm particles (Sihto *et al.* 2006). Thus, to estimate the contribution of $[\text{H}_2\text{SO}_4]$ to the growth rate of the particles between diameters 1.5 and 3 nm, we multiplied the values given by Eq. 2 with a factor of 2.5. $[\text{H}_2\text{SO}_4]$ was calculated as the average concentration between the beginning of the fast increase of $[\text{H}_2\text{SO}_4]$ and the time when concentration is more or less equal than it was before the fast increase.

Calculation of new particle formation rate $J_{1.5}$

The time evolution of the concentration N_{3-6} of particles with diameters from 3 to 6 nm can be described with a balance equation

$$\frac{dN_{3-6}}{dt} = \text{GR}_3 n_3 - \text{GR}_6 n_6 - \text{CoagS}_{3-6} N_{3-6}, \quad (3)$$

where $n_d = dN_d/dd_p$ is the particle size distribution function with the particle diameter d_p and GR_{dp} is the growth rate of the particles with diameter d_p . CoagS_{3-6} stands for the average coagulation sink for the particles with $d_p = 3-6$ nm (Kulmala *et al.* 2001), describing their scavenging on the surfaces of the present particles. Hence, the first term on the right hand side of Eq. 3 describes the growth into the size range 3–6 nm, the second term the growth out of it, and the third term the loss by the coagulation scavenging. By denoting the formation rate of 3 nm particles (the first term on the right hand side of Eq. 3) with J_3 and rearranging the terms of Eq. 3, and using approximations as outlined below, we get

$$J_3 = \frac{dN_{3-6}}{dt} + \text{CoagS}_4 N_{3-6} + \frac{N_{3-6}}{3 \text{ nm}} \text{GR}_{1.5-3}. \quad (4)$$

The approximations made to form Eq. 4 are the following: both the concentration of particles in range 3–6 nm and their growth rate from 1.5 nm to 6 nm are close to constants with respect to

particle diameter. The latter holds as the particle growth rate in the kinetic regime is almost independent of size when the vapour pressure of sulphuric acid is clearly higher than its equilibrium vapour pressure (*see e.g.* Seinfeld and Pandis 1998). Thus, we may write $n_6 = N_{3-6}/(6 \text{ nm} - 3 \text{ nm})$ and $\text{GR}_6 = \text{GR}_{1.5-3}$. Additionally, the average coagulation sink CoagS_{3-6} for 3–6 nm particles was estimated as a sink CoagS_4 for the approximate geometric mean diameter (4 nm) of the size range. The time derivative dN_{3-6}/dt was calculated with numerical derivation of the N_{3-6} data.

The nucleation rate $J_{1.5}$ was then estimated from the J_3 data by the method presented by Kerminen and Kulmala (2002)

$$J_{1.5} = J_3(t + \Delta t) \exp \left[\gamma \frac{\text{CS}'}{\text{GR}_{1.5-3}} \left(\frac{1}{1.5 \text{ nm}} - \frac{1}{3 \text{ nm}} \right) \right], \quad (5)$$

where γ is a coefficient with the approximate value of $0.23 \text{ m}^2 \text{ nm}^2 \text{ s}^{-1}$ and $\text{CS}' = \sum 0.5 d_{p,j} \beta_{M,j} N_j$ is the condensation sink in units m^{-2} , where $\beta_{M,j}$ is the Fuchs-Sutugin transitional correction factor for particles with diameter $d_{p,j}$. Actually here, CS' describes the coagulational scavenging during the growth from 1.5 nm to 3 nm and thus it is calculated as a median value during the time interval $[t, t + \Delta t]$.

Determination of parameters for activation and kinetic nucleation

In this work, we studied two nucleation theories, the activation and the kinetic theory (Kulmala *et al.* 2006, Sihto *et al.* 2006, Riipinen *et al.* 2007). These theories couple the new particle formation rate to the sulphuric acid concentration with a power-law function with linear or squared dependence on sulphuric acid.

In the activation theory (Kulmala *et al.* 2006), sulphuric acid is assumed to activate the pre-existing clusters with diameter below 2 nm for growth. Thus, the nucleation rate can be assumed to have linear dependence on the sulphuric acid concentration

$$J_{1.5} = A[\text{H}_2\text{SO}_4], \quad (6)$$

where A is the activation coefficient. This theory presumes the existence of a constant pool of

clusters with diameters of 1–2 nm. Such a pool has been observed afterwards when new measurement devices, such as NAIS (Neutral Air Ion Spectrometer) for example, have made possible the direct observation of this size class clusters (Kulmala *et al.* 2007).

The kinetic theory (McMurry and Friedlander 1979, Lushnikov and Kulmala 1998) suggests that the stable particles are formed in collisions of two sulphuric acid molecules. According to the kinetic gas theory the collision frequency of two molecules is correlated with the concentration of both molecules, which in case of two colliding sulphuric acid molecules leads to a collision frequency related to the squared sulphuric acid concentration, i.e.

$$J_{1.5} = K[\text{H}_2\text{SO}_4]^2, \quad (7)$$

where K is the kinetic coefficient. Note that we used the modified form of kinetic nucleation here: the coefficient K is a free parameter and includes both the collision frequency and the probability of the collision to form a stable particle (Weber *et al.* 1996, Sihto *et al.* 2006).

The coefficients A and K include various, hitherto unidentified physical and chemical properties of the nucleation mechanisms. We did not make any presumptions on the values or dependencies of these coefficients.

Evaluation of coefficients A and K

We compared the nucleation rate calculated from the particle size distribution data $J_{1.5}$ with predicted formation rates $J_{\text{act}} \sim [\text{H}_2\text{SO}_4]$ and $J_{\text{kin}} \sim [\text{H}_2\text{SO}_4]^2$ (Eqs. 6 and 7) to see how well the theories predict the diurnal pattern of the nucleation rate. For every event day, we evaluated the coefficients A and K by fitting the observed formation rates with those predicted by the Eqs. 6 and 7 using the method of least squares. To double-check the values, one fitting was done by comparing $J_{1.5}$ from Eq. 5 with J_{act} and J_{kin} from Eqs. 6 and 7, and another comparing the observed J_3 from Eq. 4 with J_3 's calculated from formation rates J_{act} and J_{kin} by using Eq. 5 in the reverse direction. The final values for A and K were calculated as medians of these two fittings.

A significant part of the nucleation events was observed only in particle size classes with diameters larger than 4 nm (*see* example in Fig. 1d). One possible reason for this kind of an observation is that the new particles are not formed at the measurement site itself but further upwind. Hence, the observed particles are advected to the measurement place and have had time to grow to larger sizes prior to observation. On these days the values for N_{3-6} and their time derivatives may be significantly smaller than the corresponding values at the nucleation area. This leads to an underestimation of all the other measured parameters, J_3 , $J_{1.5}$, A and K . To decide whether this underestimation was real, nine nucleation events where new particles were clearly seen in the smallest size classes were examined separately.

Comparison of coefficients A and K with other measured quantities

In addition to defining the values for A and K , we compared them with concentrations of several trace gases (SO_2 , O_3 , CO , NO , NO_2 , NO_y , H_2O_2 and ROOH) and meteorological variables (temperature, relative humidity, global and diffuse solar radiation, wind speed and direction and air pressure). The larger data set used in this study could reveal some connection which has not been found in previous studies. This comparison was made with daily values of A and K as well as with the momentary values, determined by Eqs. 6 and 7, $A = J_{1.5}/[\text{H}_2\text{SO}_4]$ and $K = J_{1.5}/[\text{H}_2\text{SO}_4]^2$.

The momentary values of $J_{1.5}$, A and K were compared with the oxidation product concentrations of several volatile organic compounds (VOC): isoprene, various monoterpenes, *p*-cymene and eucalyptol. The concentration of oxidation products of a specified VOC was estimated as

$$[\text{VOC}_{\text{ox}}] = \frac{[\text{VOC}](k_{\text{VOC,OH}}[\text{OH}] + k_{\text{VOC,O}_3}[\text{O}_3])}{\text{CS}}, \quad (8)$$

where the numerator is the production of oxidation products of the compound, in which $[\text{VOC}]$ is the concentration of the compound and $k_{\text{VOC,OH}}$ and $k_{\text{VOC,O}_3}$ are the chemical reaction rate coefficients in reactions of the VOC in question with OH and O_3 (Corchnoy and Atkinson 1990,

Atkinson 1997). CS is the condensation sink describing the loss rate of the oxidation products due to condensation in units s^{-1} . The sink is calculated as $\text{CS} = 4\pi D \text{CS}'$, where D is the diffusion coefficient for which we used the value for sulphuric acid. Thus, the value for the sink is an approximation for the respective VOC oxidation product, but the comparison between the nucleation coefficients and VOC_{ox} is still valid as the error is equal in all the data points. We would like to emphasize that the concentration described by Eq. 8 is an estimated concentration of all the oxidation products of the VOC in question. Neither the fraction of incondensable oxidation products is taken into account, nor the chemical reactions that may remove some part of VOC_{ox} from the atmosphere.

Terpene concentrations have been measured at Hohenpeissenberg since the beginning of the year 2000. Because $J_{1.5}$, A and K were determined only on event days, there were only 10 days (all together 42 data points) when the comparison between these quantities and estimated VOC oxidation product concentrations $[\text{VOC}_{\text{ox}}]$ was possible. Because the time resolution of VOC measurements was 20 minutes, we calculated the corresponding values for $J_{1.5}$, A and K as an average of the data points within that time interval. Only those VOC measurements were taken into account during which the concentrations of most of the terpenes were above the detection limit (24 data points).

Results and discussion

Our general results concerning the frequency of particle formation events, the formation and growth rates of the new particles were widely consistent with the previous analysis by Birmili *et al.* (2003). In this study we describe in more detail the connection between the particle formation rate and the gaseous sulphuric acid concentration.

Classification of the days

The total number of days with enough particle size distribution data to make the event

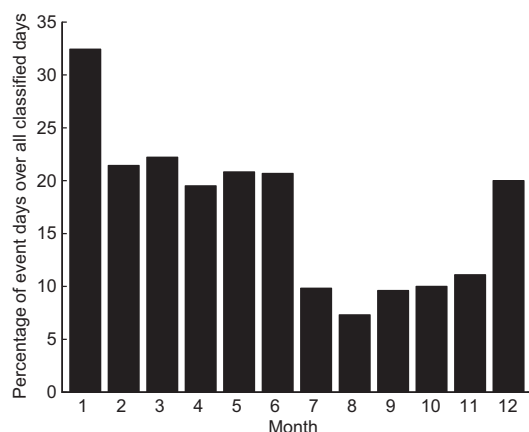


Fig. 2. Monthly percentage of event days over the sum of event and non-event days.

classification was 595. Out of those days 99 were event days, 114 were undefined and 369 were non-event days. Interestingly the event frequency exhibited a maximum in winter (Fig. 2). This was surprising, because at several other continental areas the highest event frequency is observed in spring or summer time (Mäkelä *et al.* 2000, Birmili *et al.* 2001, Dal Maso *et al.* 2005, Hamed *et al.* 2006). For the HAFEX data, both the event frequencies and their seasonal variation agreed very well with the previous analysis of Birmili *et al.* (2003), who classified the days with numeric method based on the histories of total and ultrafine (3–11 nm) particle concentrations.

The determination of Δt and $GR_{1.5-3}$

The time interval Δt , during which the diameter of the nucleated particles grows to 3 nm, was determined from changes in sulphuric acid concentration $[H_2SO_4]$ and in concentration of particles with diameters from 3 to 6 nm (N_{3-6}) (an example of the fitting procedure is shown in Fig. 3). The data for both $[H_2SO_4]$ and N_{3-6} were sufficient for determining Δt on 52 out of 99 classified event days.

The median of the time delays was 20 min (Fig. 4) corresponding to the growth rate $GR_{1.5-3} \approx 4.5 \text{ nm h}^{-1}$ (Eq. 1). On 85% of the event days, Δt was 1.0 h or smaller ($GR_{1.5-3} \geq 1.5 \text{ nm h}^{-1}$). On 7 days, corresponding to 13% of the

studied events, the time delay was 0 h, which means it was smaller than the time resolution of the measurements (10 min) i.e. $GR_{1.5-3} > 9 \text{ nm h}^{-1}$. The time delays were significantly shorter, and growth rates higher, than those measured in QUEST II (Sihto *et al.* 2006) and BACCI/QUEST IV campaigns in Hyytiälä and QUEST III campaign in Heidelberg (Riipinen *et al.* 2007), where the median delays were 1.7 h, 1.5 h and 1.5 h, and the corresponding median growth rates $GR_{1.5-3}$ were 0.9 nm h^{-1} , 1.0 nm h^{-1} and 1.0 nm h^{-1} , respectively.

The measured growth rate was usually significantly higher than the growth rate that would be predicted from the sulphuric acid concentration (Eq. 2). The calculated fraction of the growth related to sulphuric acid was on median 14% of the measured growth rate. On 5 out of 52 event days, $[H_2SO_4]$ could explain the growth completely. The fraction increased, on average, with increasing sulphuric acid concentration. These numbers indicate that on most days $[H_2SO_4]$ cannot explain the growth of the freshly nucleated particles alone.

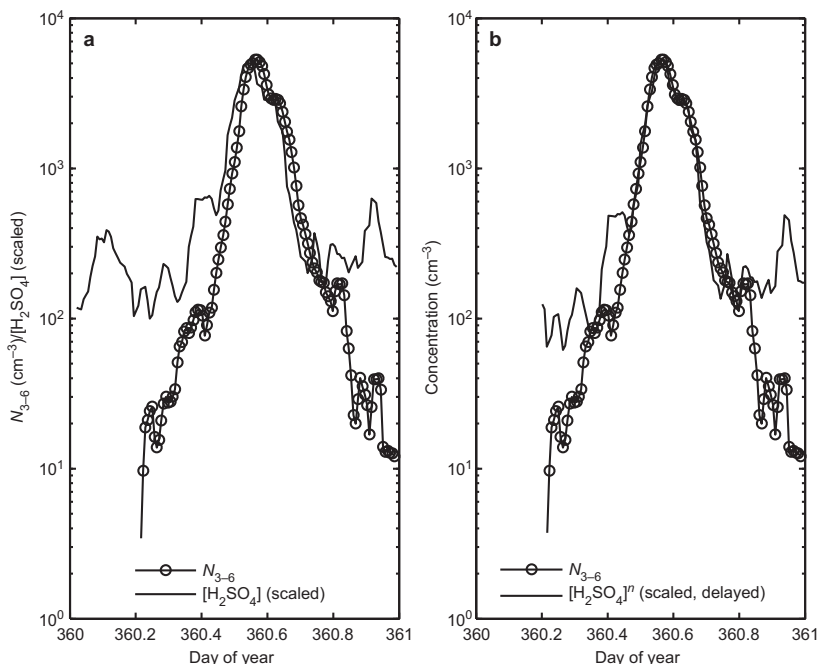
Formation rate of 1.5 nm particles and its dependence on sulphuric acid concentration

Out of the 52 event days with sufficient data for the analysis, $J_{1.5}$ was determined for those 45 days when $\Delta t > 0$ (see Eq. 5). We found a clear correlation between $[H_2SO_4]^n$ and both N_{3-6} and $J_{1.5}$ with $n = 1-2$ (Fig. 5).

We calculated the median for new particle formation rate $J_{1.5}$ during the nucleation event, taking into account the values from one hour before to one hour after the maximum formation rate. The median of all event-specific values of $J_{1.5}$ was $1.4 \text{ cm}^{-3} \text{ s}^{-1}$, with quartiles at $0.6 \text{ cm}^{-3} \text{ s}^{-1}$ and $2.7 \text{ cm}^{-3} \text{ s}^{-1}$. The values did not show a seasonal pattern.

To compare which of the exponents $n = 1$ or $n = 2$ gives better approximation for $J_{1.5}$ we plotted figures with three different $J_{1.5}$ -curves (Fig. 6): one calculated from the particle data with Eq. 5 and one for both of the investigated nucleation theories (Eqs. 6 and 7) from the sulphuric acid data. The event days were divided visually into

Fig. 3. (a) An example of the fitting made to determine Δt , the time it takes for nucleated particles to reach the detectable diameter of 3 nm. Number concentration N_{3-6} of particles with a diameter 3–6 nm and sulphuric acid concentration ($[\text{H}_2\text{SO}_4]$) for 26 Dec. 1998. (b) $[\text{H}_2\text{SO}_4]$ -curve delayed by the time shift $\Delta t = 0.5$ h and raised to the power $n = 1.12$ ($R = 0.99135$). $[\text{H}_2\text{SO}_4]$ has been scaled in both figures to have the same maximum value as N_{3-6} .



two groups: group A: activation days, when $J_{1.5}$ was mainly linearly correlated to $[\text{H}_2\text{SO}_4]$ and group K: kinetic days, when $J_{1.5}$ was mainly correlated to $[\text{H}_2\text{SO}_4]^2$.

The division into A- and K-days was based on the overall behaviour of $J_{1.5}$ and $[\text{H}_2\text{SO}_4]$ during the day and the short-term deviations were ignored. However, on several A-days the exponent $n = 1$, that gave the strongest correlation for the entire day, was clearly too small to connect $J_{1.5}$ and $[\text{H}_2\text{SO}_4]$ in the very beginning of the event. Therefore, all the days were furthermore classified by the best exponent n_{beg} for the beginning of the event. Examples of A-days with $n_{\text{beg}} = 1$ and $n_{\text{beg}} \approx 2$, and K-days with $n_{\text{beg}} = 2$ are presented in Fig. 6. The result of the classification is shown in Table 1. There were six days that could not be classified in any of the categories.

The examined event days were roughly categorized as follows: 18% (7/39) of the days were A-days with $n_{\text{beg}} = 1$ and 38% (15/39) A-days with $n_{\text{beg}} \approx 2$, and 41% (16/39) were K-days.

We also examined if a correlation between $J_{1.5}$ and $[\text{OH}]$ would be stronger than the $[\text{H}_2\text{SO}_4]$ correlation. Practically on all the event days the $[\text{OH}]$ correlation was weaker and never clearly stronger than the $[\text{H}_2\text{SO}_4]$ correlation.

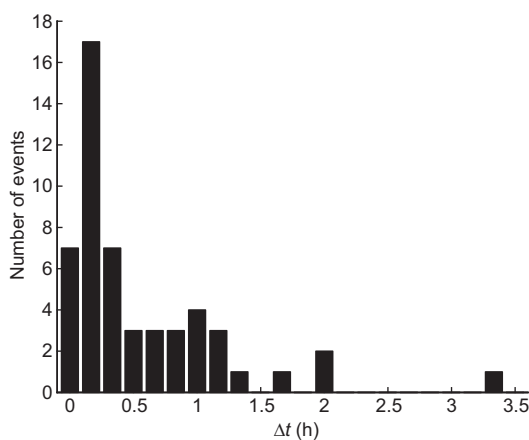


Fig. 4. Time delays (Δt) between particle formation (assumed diameter of freshly formed particle $d_{\text{nuc1}} = 1.5$ nm) and reaching the detection limit at 3 nm.

Table 1. The event days classified by the better correlation of $J_{1.5}$ to $[\text{H}_2\text{SO}_4]$ (A-days) or to $[\text{H}_2\text{SO}_4]^2$ (K-days) and the best correlation for the exponent at the very beginning of the event (n_{beg}).

	A-days	K-days	Total
$n_{\text{beg}} = 1$	7	1	8
$n_{\text{beg}} \approx 2$	15	16	31
Total	22	17	39

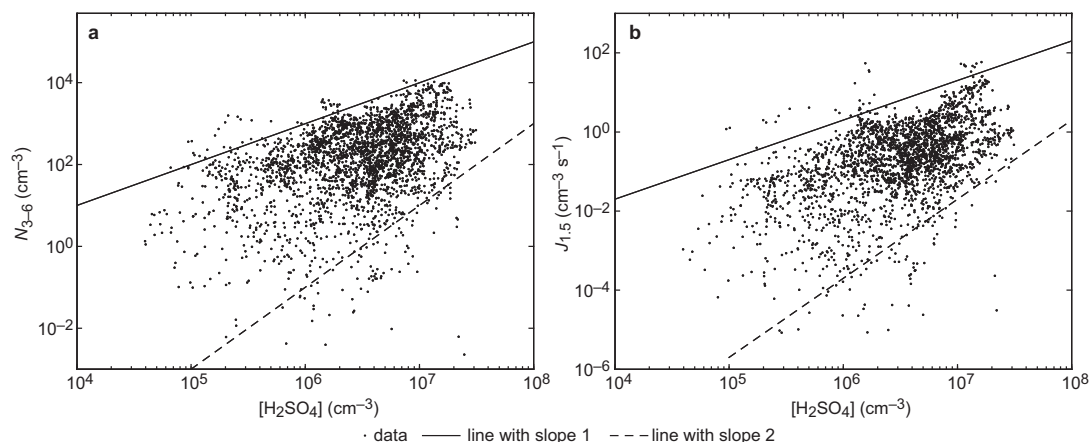


Fig. 5. (a) Concentration N_{3-6} of particles with a diameter 3–6 nm, and (b) the new particle formation rate $J_{1.5}$ estimated from the particle measurements vs. sulphuric acid concentration for all data on event days between 06:00 and 18:00. Lines represent the slopes with $n = 1$ and $n = 2$ in $[H_2SO_4]^n$.

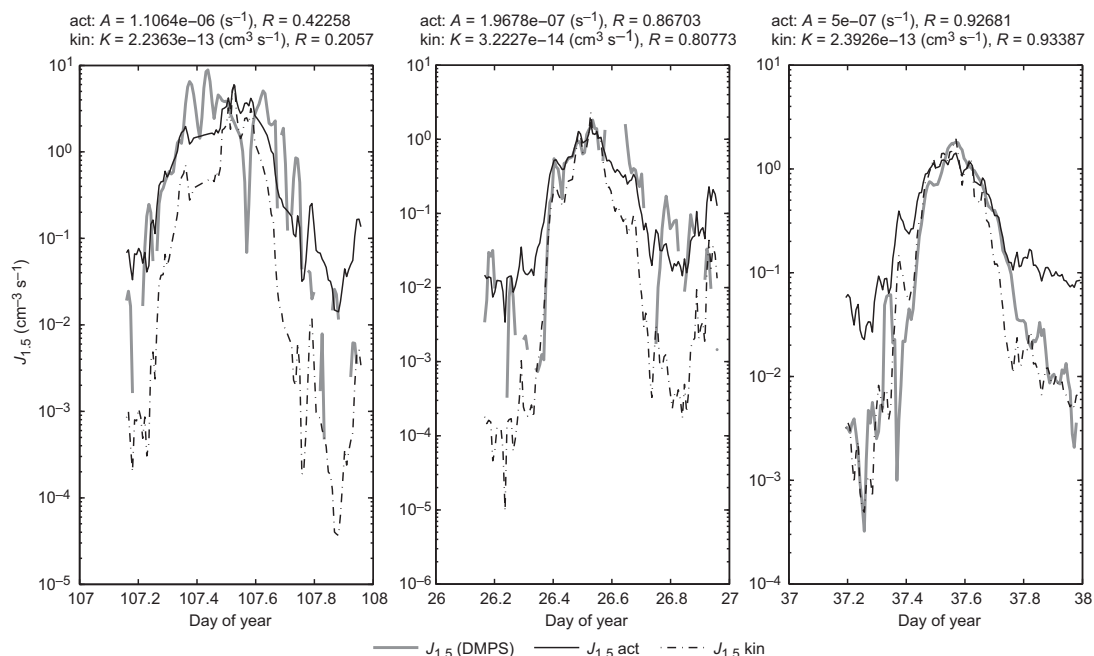


Fig. 6. Examples of the classification of event days as A-days (activation theory) or K-days (kinetic theory) (results in Table 1), according to the better correlations (for details see text): (a) A-day with $n_{\text{beg}} = 1$, (b) A-day with $n_{\text{beg}} = 2$, and (c) K-day with $n_{\text{beg}} = 2$, where n_{beg} refers to the best correlating exponent in $J_{1.5} \sim [H_2SO_4]^{n_{\text{beg}}}$ for the beginning of the event.

A and K

The definition of the values of activation and kinetic coefficient was made by performing a least squares fit between $J_{1.5}$ calculated from DMPS measurements with Eqs. 2–4 and from sulphuric

acid concentration with Eqs. 6 and 7. The median of the daily activation coefficients A was $1.6 \times 10^{-7} \text{ s}^{-1}$ with the quartiles at $7.5 \times 10^{-8} \text{ s}^{-1}$ and $3.0 \times 10^{-7} \text{ s}^{-1}$. The median of the daily kinetic coefficients K was $3.2 \times 10^{-14} \text{ cm}^3 \text{ s}^{-1}$ with the quartiles at $9.4 \times 10^{-15} \text{ cm}^3 \text{ s}^{-1}$ and $6.2 \times 10^{-14} \text{ cm}^3 \text{ s}^{-1}$. In

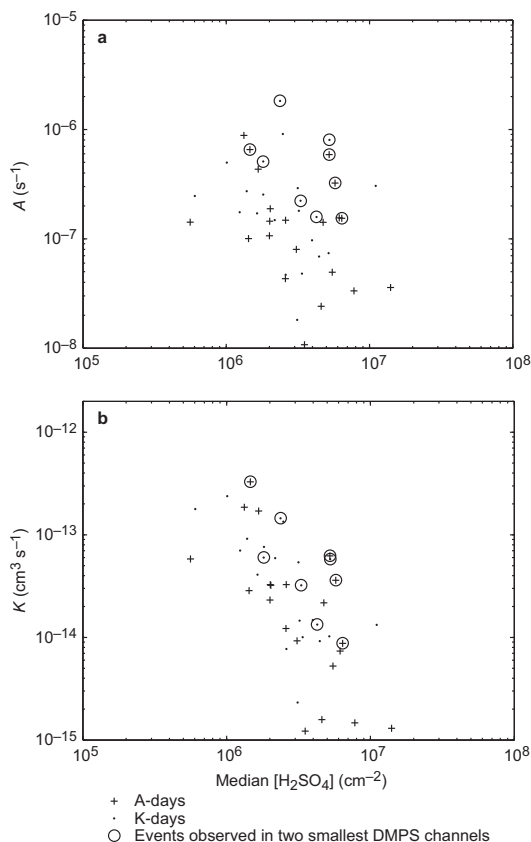


Fig. 7. Daily values of (a) the activation coefficient A and (b) the kinetic coefficient K vs. median sulphuric acid concentration during the event. On circled days the event was observed also in the two smallest size channels of the DMPS.

these median and quartile values all the days were taken into account despite their classification as A- or K-days, since the days with different categories did not show different behaviour in terms of values of the coefficients or their dependence on [H₂SO₄].

When we took into account only the nine days when nucleation events were observed also in the two smallest size channels of the DMPS, the values for the coefficients (A_{3-4} and K_{3-4}) increased a little. The median for A_{3-4} was $5.1 \times 10^{-7} \text{ s}^{-1}$ and for K_{3-4} $5.8 \times 10^{-14} \text{ cm}^3 \text{ s}^{-1}$.

The value of A did not correlate with the median sulphuric acid concentration during the event (Fig. 7a). Instead, the value of K showed an anticorrelation with the median [H₂SO₄] (Fig.

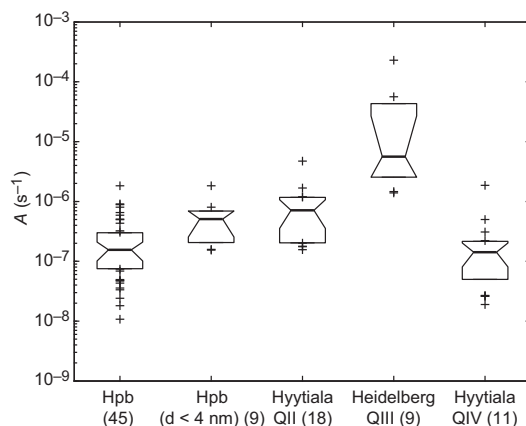


Fig. 8. Comparison of medians (bold lines) and quartiles (boxes) of activation coefficient values in Hohenpeissenberg (Hpb) and in QUEST campaigns in Hyytiälä (QUEST II in 2003 and BACCI/QUEST IV in 2005) and Heidelberg (QUEST III in 2004). The number of event days used in analysis is presented in parentheses. The first box on the left (Hpb) is for all analysed event days in Hohenpeissenberg and the second (Hpb, particle diameter < 4 nm) for the days on which the event was observed also in the two smallest size channels of the DMPS. Crosses represent the measurements outside the quartiles.

7b). This was also observed for A_{3-4} and K_{3-4} , though defining the correlation from only 9 points does not produce a statistically relevant result. Because the correlation between A and [H₂SO₄] was not positive and $K \sim A/[\text{H}_2\text{SO}_4]$ (Eqs. 6 and 7), the anticorrelation of K was expected.

We compared the median and quartile values of the activation coefficient A with the corresponding values (Fig. 8) for QUEST II and BACCI/QUEST IV campaigns in Hyytiälä and QUEST III campaign in Heidelberg (Sihto *et al.* 2006, Riipinen *et al.* 2007). The A values for QUEST campaigns shown in Fig. 8 are not exactly the same as those given in the references, because there the formation rates were calculated for particles with diameter 1 nm. Hence, the values for Hyytiälä and Heidelberg were recalculated with $J_{\text{nucl}} = J_{1.5}$. The A values were quite similar in Hohenpeissenberg and in Hyytiälä ($A \approx 10^{-8}$ – 10^{-6} s^{-1}), but in Heidelberg A was about two orders of magnitude higher. The reason for this difference has not been explained yet. For the K values the results were similar (not shown).

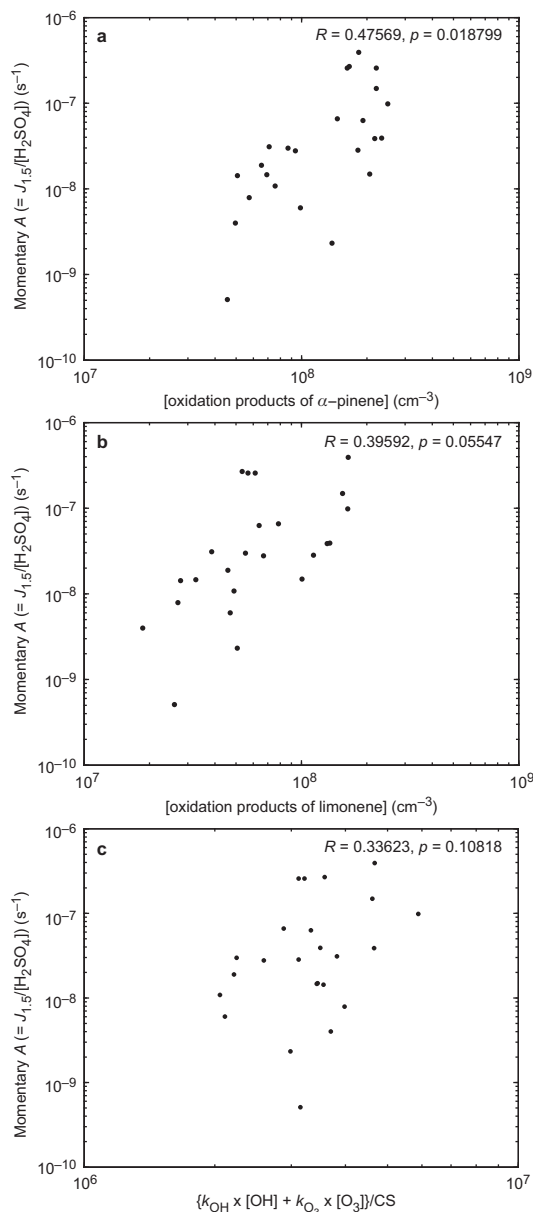


Fig. 9. Momentary values of activation coefficient A vs. oxidation product concentration of (a) α -pinene, (b) limonene, and (c) the multiplier $(k_{\text{OH}}[\text{OH}] + k_{\text{O}_3}[\text{O}_3])/\text{CS}$ as oxidation potential. Only the data for which the concentrations of most of the VOCs were above the detection limit (24 data points) are shown.

Comparison of A , K and $J_{1.5}$ with oxidation products of VOCs and other variables

The observed variations in the daily values of A

and K could not be linked to the corresponding variations of meteorological variables (temperature, relative humidity, diffuse solar and global radiation, wind speed and direction, and air pressure) or gas concentrations (SO_2 , O_3 , CO , NO , NO_2 , NO_y , H_2O_2 and ROOH).

As no perfect correlations between $J_{1.5}$ and $[\text{H}_2\text{SO}_4]^n$ were achieved with the daily coefficients, some variable or variables might explain the fluctuations of the particle formation rate out of that predicted in Eqs. 6 and 7. Therefore, we made the same comparisons also with momentary values of A and K , meaning the values given by Eqs. 6 and 7, $A = J_{1.5}/[\text{H}_2\text{SO}_4]$ and $K = J_{1.5}/[\text{H}_2\text{SO}_4]^2$. We compared the momentary values of coefficients A and K with meteorological variables and gas concentrations, but still no significant correlations were found.

Instead, the momentary values of A and K showed correlations with the estimated concentrations of terpene oxidation products $[\text{VOC}_{\text{ox}}]$ as calculated with Eq. 8 (Fig. 9a, b and Table 2).

The highest correlation coefficient between A and $[\text{VOC}_{\text{ox}}]$ was found for α -pinene ($R = 0.48$ and $p = 1.9 \times 10^{-2}$; p is the probability of obtaining the observed or better correlation by coincidence) and between K and $[\text{VOC}_{\text{ox}}]$ for myrcene ($R = 0.73$ and $p = 1.8 \times 10^{-4}$). The strongest correlations were observed for monoterpenes emitted from coniferous trees (in Table 2 from myrcene down to limonene; Andreani-Aksoyoglu and Keller 1995) whereas weaker correlations were found for those monoterpenes emitted by the most abundant deciduous tree species around the site, European beech (γ -terpinene and sabinene; Dindorf *et al.* 2005). It is worth mentioning that the correlations between coefficients A or K and $[\text{VOC}_{\text{ox}}]$ related to coniferous trees were stronger than those between A or K and the multiplier $(k_1[\text{OH}] + k_2[\text{O}_3])/\text{CS}$ (see Eq. 8), which can roughly be interpreted as an oxidation potential (see Fig. 9c). This means that the concentrations of the oxidizers alone cannot explain the observed correlations. Here k_{OH} and k_{O_3} are average values of the reaction rate coefficients of different VOCs with OH and O_3 .

Additionally, we compared the momentary values of $J_{1.5}$ with $[\text{VOC}_{\text{ox}}]$ (see Table 2). The correlations were clearly stronger between A or K and $[\text{VOC}_{\text{ox}}]$ than between $J_{1.5}$ and $[\text{VOC}_{\text{ox}}]$

for all the VOCs for which $R > 0.3$. Due to the same kind of diurnal pattern of $J_{1.5}$ and $[\text{VOC}_{\text{ox}}]$, we might see a correlation between them even if there was no true connection between $[\text{VOC}_{\text{ox}}]$ and new particle formation. On the other hand, because also $[\text{H}_2\text{SO}_4]$ has a similar diurnal pattern as $J_{1.5}$, $A (= J_{1.5}/[\text{H}_2\text{SO}_4])$ is expected to have a less pronounced diurnal pattern than $J_{1.5}$, and $K (= J_{1.5}/[\text{H}_2\text{SO}_4]^2 \sim [\text{H}_2\text{SO}_4]^{n-2}$ with $n \leq 2$, since $J_{1.5} \sim [\text{H}_2\text{SO}_4]^n$) is expected to show either no diurnal pattern at all or an inverted diurnal pattern compared to $J_{1.5}$. As demonstrated, A and K correlate better with $[\text{VOC}_{\text{ox}}]$ than with $J_{1.5}$. This seems to indicate a connection between $[\text{VOC}_{\text{ox}}]$ and new particle formation. No significantly better correlation is observed with either of the theories, thus, based on this analysis with a very restricted number of VOC data, there is no preference found for activation or kinetic theory.

Conclusions

In this work, the comprehensive data set of atmospheric particle size distributions and sulphuric acid concentrations collected 1998–2000 at Hohenpeissenberg (HAFEX) was re-analysed with respect to the occurrences of new particle formation, and with new analyses added to investigate the plausibility of the activation-

type or the kinetic-type nucleation theory. Our phenomenological analysis of the seasonal frequency of particle formation events showed a maximum in winter, in analogy to the initial work by Birmili *et al.* (2003). This observation deviates substantially from the seasonal event frequency observed in lowland measurement sites, where the event frequency has a minimum in winter (e.g. Mäkelä *et al.* 2000, Birmili *et al.* 2001, Dal Maso *et al.* 2005, Hamed *et al.* 2006). The median particle formation rate on the event days was $1.4 \text{ cm}^{-3} \text{ s}^{-1}$. The median particle growth rate from 1.5 nm to 3 nm was 4.5 nm h^{-1} and the median theoretical contribution of sulphuric acid concentration to the observed growth was 14%. The nucleation mode growth rates at Hohenpeissenberg were more than four times higher than those measured in Hyytiälä and Heidelberg (Sihto *et al.* 2006, Riipinen *et al.* 2007). This difference remains unexplained.

We were able to show that the particle formation rate during nucleation events in the atmospheric boundary layer can be described by a power law function of sulphuric acid concentration $J_{1.5} \sim [\text{H}_2\text{SO}_4]^n$, with n between 1 and 2. This is in agreement with previous investigations at other continental observation sites (Sihto *et al.* 2006, Riipinen *et al.* 2007). However, in most cases the exponent had values close to two at the beginning of an event but values rather close

Table 2. Correlation coefficients between the concentration of oxidation products of VOCs and nucleation rate, activation coefficient and kinetic coefficient. Coefficients for the sum of the oxidation product concentrations and for $(k_{\text{OH}}[\text{OH}] + k_{\text{O}_3}[\text{O}_3])/\text{CS}$ describing the oxidation potential are also presented.

Compound	$R (J_{1.5}, [\text{VOC}_{\text{ox}}])$	$R (A, [\text{VOC}_{\text{ox}}])$	$R (K, [\text{VOC}_{\text{ox}}])$
α -pinene	0.32	0.48	0.43
Camphene	0.31	0.47	0.51
β -pinene	0.19	0.45	0.44
Myrcene	0.14	0.43	0.73
3-carene	0.12	0.41	0.47
Limonene	0.07	0.40	0.59
Tricyclene	0.26	0.38	0.38
<i>p,m</i> -xylene	0.15	0.29	0.50
γ -terpine	-0.06	0.25	0.41
Sabinene	-0.01	0.17	0.23
Isoprene	0.15	0.15	0.10
<i>p</i> -cymene	0.18	0.44	0.47
Eucalyptol	0.30	0.41	0.43
Sum of $[\text{VOC}_{\text{ox}}]$	0.18	0.47	0.53
$(k_{\text{OH}}[\text{OH}] + k_{\text{O}_3}[\text{O}_3])/\text{CS}$	0.14	0.34	0.38

to one for the rest of the day. Calculations of the activation coefficients A for each nucleation event day yielded a median value $1.6 \times 10^{-7} \text{ s}^{-1}$. The median value for kinetic coefficient K was $3.2 \times 10^{-14} \text{ cm}^{-3} \text{ s}^{-1}$. The daily values of the coefficients varied within two orders of magnitude and also during the events the observed formation rates fluctuated around the rates predicted from the sulphuric acid concentration. Neither daily nor momentary values of A and K were found to correlate with measured meteorological variables or trace gas concentrations. The values of A and K agreed well with the previous results, especially with those from the rural site in Hyytiälä (Sihto *et al.* 2006, Riipinen *et al.* 2007). The values determined for A and K at a semi-urban site in Heidelberg were about one order of magnitude higher (Riipinen *et al.* 2007).

The median sulphuric acid concentration during the event did not have a significant effect on A , but K was weakly anticorrelated with the median sulphuric acid concentration. This finding supports the activation theory but does not support the kinetic theory, as the coefficients should not be dependent on sulphuric acid concentration. Nevertheless, on significant part of the event days the nucleation rate correlated better with $[\text{H}_2\text{SO}_4]^n$ with $n = 2$ than with $n = 1$. This could be explained by the nucleation rate being linearly connected both to sulphuric acid concentration and another unknown parameter with a similar diurnal pattern.

We observed a visual correlation between the momentary values of A and K , and the estimated concentrations of monoterpene oxidation products. The correlation was significantly stronger with the terpenes emitted from the coniferous trees than with those originating from the deciduous trees. The higher values of the coefficients A and K in Heidelberg observed in an earlier study (Riipinen *et al.* 2007) might thus be explained with higher volatile organic compound concentrations. Previously the contribution of the organic vapours to new particle formation has been predicted by e.g. Kulmala *et al.* (2004b), but not observed in simple correlations (Birmili *et al.* 2003). Our results suggest that oxidation products of VOCs are involved in the first steps of new particle formation. They also show a diurnal pattern similar to sulphuric

acid and could therefore explain the observed daily values between 1 and 2 for exponent n in relation $J_{1.5} \sim [\text{H}_2\text{SO}_4]^n$. As the observed correlations between nucleation coefficients and monoterpene oxidation products are based on a rather small number of data points, further research is needed to describe more accurately the role of VOCs in new particle formation.

Acknowledgements: Financial support from the Academy of Finland Centre of Excellence program (project nos. 211483, 211484 and 1118615) and the Maj and Tor Nessling Foundation is gratefully acknowledged.

References

- Andreani-Aksoyoglu S. & Keller J. 1995. Estimates of monoterpene and isoprene emissions from the forests in Switzerland. *J. Atmos. Chem.* 20: 71–87.
- Atkinson R. 1997. Gas-phase tropospheric chemistry of volatile organic compounds: 1. Alkanes and alkenes. *J. Phys. Chem. Ref. Data* 26: 215–290.
- Berresheim H., Elste T., Plass-Dülmer C., Eisele F.L. & Tanner D.J. 2000. Chemical ionization mass spectrometer for long-term measurements of atmospheric OH and H_2SO_4 . *Int. J. Mass Spectrom.* 202: 91–109.
- Birmili W., Stratmann F. & Wiedensohler A. 1999. Design of a DMA-based size spectrometer for large particle size range and stable operation. *J. Aerosol Sci.* 30: 549–554.
- Birmili W., Wiedensohler A., Heintzenberg J. & Lehmann K. 2001. Atmospheric particle number size distribution in central Europe: Statistical relations to air masses and meteorology. *J. Geophys. Res.* 106: 32005–32018.
- Birmili W., Berresheim H., Plass-Dülmer C., Elste T., Gilge S., Wiedensohler A. & Uhrner U. 2003. The Hohenpeissenberg aerosol formation experiment (HAFEX): a long-term study including size-resolved aerosol, H_2SO_4 , OH and monoterpenes measurements. *Atmos. Chem. Phys.* 3: 361–376.
- Cabada J.C., Khlystov A., Wittig A.E., Pilinis C. & Pandis S.N. 2004. Light scattering by fine particles during the Pittsburgh Air Quality Study: measurements and modeling. *J. Geophys. Res.* 109, D16S03, doi:10.1029/2003JD004155.
- Corchnoy S.B. & Atkinson R. 1990. Kinetics of the gas-phase reactions of OH and NO_3 radicals with 2-carene, 1,8-cineole, *p*-cymene, and terpinolene. *Environ. Sci. Technol.* 24: 1497–1502.
- Dal Maso M., Kulmala M., Riipinen I., Wagner R., Hussein T., Aalto P.P. & Lehtinen K.E.J. 2005. Formation and growth of fresh atmospheric aerosols: eight years of aerosol size distribution data from SMEAR II, Hyytiälä, Finland. *Boreal Env. Res.* 10: 323–336.
- Dindorf T., Kuhn U., Ganzeveld L., Schebeske G., Ciccioli P., Holzke C., Köble R., Seufert G. & Kesselmeier J. 2005. Emission of monoterpenes from European beech

- (*Fagus sylvatica* L.) as a function of light and temperature. *Biogeosciences Discussions* 2: 137–182.
- Dockery D.W. & Pope C.A. 1994. Acute respiratory effects of particulate air pollution. *Annual Review of Public Health* 15: 107–132.
- Hamed A., Joutsensaari J., Mikkonen S., Sogacheva L., Dal Maso M., Kulmala M., Cavalli F., Fuzzi S., Facchini M.C., Decesari S., Mircea M., Lehtinen K.E.J. & Laaksonen A. 2007. Nucleation and growth of new particles in Po Valley, Italy. *Atmos. Chem. Phys.* 7: 355–376.
- Kerminen V.-M. & Kulmala M. 2002. Analytical formulae connecting the “real” and “apparent” nucleation rate and the nuclei number concentration for atmospheric nucleation events. *J. Aerosol Sci.* 33: 609–622.
- Korhonen H., Lehtinen K.E.J. & Kulmala M. 2004. Multicomponent aerosol dynamics model UHMA: model development and validation. *Atmos. Chem. Phys.* 4: 757–771.
- Kuang C., McMurry P.H., McCormick A.V. & Eisele F.L. 2008. Dependence of nucleation rates on sulfuric acid vapor concentration in diverse atmospheric locations. *J. Geophys. Res.* 113, D10209, doi:10.1029/2007JD009253.
- Kulmala M., Dal Maso M., Mäkelä J.M., Pirjola L., Väkevä M., Aalto P.P., Mikkulainen P., Hämeri K. & O’Dowd C.D. 2001. On the formation, growth and composition of nucleation mode particles. *Tellus* 53B: 479–490.
- Kulmala M., Vehkamäki H., Petäjä T., Dal Maso M., Lauri A., Kerminen V.-M., Birmili W. & McMurry P.H. 2004a. Formation and growth rates of ultrafine atmospheric particles: a review of observations. *J. Aerosol Sci.* 35: 146–176.
- Kulmala M., Suni T., Lehtinen K.E.J., Dal Maso M., Boy M., Reissell A., Rannik Ü., Aalto P., Keronen P., Hakola H., Bäck J., Hoffmann T., Vesala T. & Hari P. 2004b. A new feedback mechanism linking forests, aerosols, and climate. *Atmos. Chem. Phys.* 4: 557–562.
- Kulmala M., Lehtinen K.E.J. & Laaksonen A. 2006. Cluster activation theory as an explanation of the linear dependence between formation rate of 3 nm particles and sulphuric acid concentration. *Atmos. Chem. Phys.* 6: 787–793.
- Kulmala M., Riipinen I., Sipilä M., Manninen H.E., Petäjä T., Junninen H., Dal Maso M., Mordas G., Mirme A., Vana M., Hirsikko A., Laakso L., Harrison R.M., Hanson I., Leung C., Lehtinen K.E.J. & Kerminen V.-M. 2007. Toward direct measurement of atmospheric nucleation. *Science* 318: 89–92.
- Lehtinen K.E.J. & Kulmala M. 2003. A model for particle formation and growth in the atmosphere with molecular resolution in size. *Atmos. Chem. Phys.* 3: 251–257.
- Lushnikov A. & Kulmala M. 1998. Dimers in nucleating vapors. *Phys. Rev. E* 58: 3157–3167.
- McMurry P. & Friedlander S.K. 1979. New particle formation in the presence of an aerosol. *Atmos. Environ.* 13: 1635–1651.
- Mäkelä J.M., Dal Maso M., Pirjola L., Keronen P., Laakso L., Kulmala M. & Laaksonen A. 2000. Characteristics of the atmospheric particle formation events observed at a boreal forest site in southern Finland. *Boreal Env. Res.* 5: 299–313.
- Napari I., Noppel M., Vehkamäki H. & Kulmala M. 2002. An improved model for ternary nucleation of sulfuric acid — ammonia — water. *J. Chem. Phys.* 116: 4221–4227.
- Pope C.A.III, Burnett R.T., Thun M.J., Calle E.E., Krewski D., Ito K. & Thurston G.D. 2002. Lung cancer, cardiovascular mortality, and long-term exposure to fine particulate air pollution. *Journal of the American Medical Association* 287: 1132–1141.
- Ramanathan V. 2007. Global and regional climate change: the next few decades. *Developments in Earth Surface Processes* 10: 9–11.
- Riipinen I., Sihto S.-L., Kulmala M., Arnold F., Dal Maso M., Birmili W., Saarnio K., Teinilä K., Kerminen V.-M., Laaksonen A. & Lehtinen K.E.J. 2007. Connections between atmospheric sulphuric acid and new particle formation during QUEST III–IV campaigns in Heidelberg and Hyytiälä. *Atmos. Chem. Phys.* 7: 1899–1914.
- Seinfeld J.H. & Pandis S.N. 1998. *Atmospheric chemistry and physics*. John Wiley & Sons, New York.
- Sihto S.-L., Kulmala M., Kerminen V.-M., Dal Maso M., Petäjä T., Riipinen I., Korhonen H., Arnold F., Janson R., Boy M., Laaksonen A. & Lehtinen K.E.J. 2006. Atmospheric sulphuric acid and aerosol formation: implications from atmospheric measurements for nucleation and early growth mechanisms. *Atmos. Chem. Phys.* 6: 4079–4091.
- Sihto S.-L., Vuollekoski H., Leppä J., Riipinen I., Kerminen V.-M., Korhonen H., Lehtinen K.E.J., Boy M. & Kulmala M. 2009. Aerosol dynamics simulations on the connection of sulphuric acid and new particle formation. *Atmos. Chem. Phys.* 9: 2933–2947.
- Spracklen D.V., Carslaw K.S., Kulmala M., Kerminen V.-M., Mann G.W. & Sihto S.-L. 2006. The contribution of boundary layer nucleation events to total particle concentrations on regional and global scales. *Atmos. Chem. Phys.* 6: 5631–5648.
- Spracklen D.V., Carslaw K.S., Kulmala M., Kerminen V.-M., Sihto S.-L., Riipinen I., Merikanto J., Mann G.W., Chipperfield M.P., Wiedensohler A., Birmili W. & Lihavainen H. 2008. Contribution of particle formation to global cloud condensation nuclei concentrations. *Geophys. Res. Lett.* 35, L06808, doi:10.1029/2007GL033038.
- Vehkamäki H., Kulmala M., Napari I., Lehtinen K.E.J., Timmreck C., Noppel M. & Laaksonen A. 2002. An improved parameterization for sulfuric acid–water nucleation rates for tropospheric and stratospheric conditions. *J. Geophys. Res.* 107, 4622, doi:10.1029/2002JD002184.
- Weber R.J., McMurry P.H., Eisele F.L. & Tanner D.J. 1995. Measurement of expected nucleation precursor species and 3–500 nm diameter particles at Mauna Loa Observatory, Hawaii. *J. Atmos. Sci.* 52: 2242–2257.
- Weber R.J., Marti J.J., McMurry P.H., Eisele F.L., Tanner D.J. & Jefferson A. 1997. Measurements of new particle formation and ultrafine particle growth rates at a clean continental site. *J. Geophys. Res.* 102: 4375–4385.
- Zhang M. & Wexler A. 2004. Evolution of particle number distribution near roadways, Part I: analysis of aerosol dynamics and its implications for engine emission measurement. *Atmos. Environ.* 38: 6643–6653.